IEEE Access
Multidisciplinary ⋮ Rapid Review ⋮ Open Access Journal

Received February 24, 2018, accepted April 13, 2018, date of publication May 16, 2018, date of current version June 26, 2018.

Digital Object Identifier 10.1109/ACCESS.2018.2837082

# A Distributed Voltage Control Strategy for Multi-Microgrid Active Distribution Networks Considering Economy and Response Speed

**XIAOBO DOU[1], (Member, IEEE), PEI XU[1], QINRAN HU[2], (Member, IEEE), WANXING SHENG[3], (Senior Member, IEEE), XIANGJUN QUAN[1], (Student Member, IEEE), ZAIJUN WU[1], (Member, IEEE), AND BIN XU[4]**

[1]School of Electrical Engineering, Southeast University, Nanjing 210096, China
[2]School of Engineering and Applied Sciences, Harvard University, Cambridge, MA 02138, USA
[3]China Electric Power Research Institute, Beijing 100192, China
[4]State Grid Anhui Electric Power Corporation Research Institute, Hefei 230000, China

Corresponding author: Xiaobo Dou (dxb_2001@sina.com)

This work was supported in part by the National Natural Science Foundation of China under Grant 51777031 and in part by the National Key Research and Development Plan of China under Grant 2016YFB0900400.

**ABSTRACT** This paper presents a novel distributed voltage control strategy to maintain the voltage of active distribution networks containing multiple microgrids. Local voltage regulation characteristics, such as power reserve, adjustment cost, and regulating speed, are identified first. According to a neighbors' voltage regulation characteristics, the microgrid coordinates neighborhood resources and asks them for coordination as soon as voltage problems occur. Microgrids schedule local resources based on a cooperative distributed model predictive control algorithm scheme with neighbor-to-neighbor communication. Tests are performed in an active distribution network with three microgrids. The numerical studies have shown that the proposed strategy mitigates the voltage fluctuation rapidly and efficiently with minimum operating cost.

**INDEX TERMS** Active distribution networks, distributed generation, distributed model predictive control, voltage control.

## I. INTRODUCTION

As the penetration of distributed generations (DGs) grow in distribution networks, the characteristic of a distribution network is becoming similar to an active transmission network, which is called active distribution network (ADN) [1]. The implementation of DGs in ADNs promises many benefits, such as power loss reduction and a decrease in environmental pollution levels. However, the output of DGs, especially renewables, are prone to intermittency, randomness and uncertainty, which will cause voltage fluctuation and power quality disturbances if there are no reasonable controls [2]. Typical control actions, such as On-Load Tap Changers (OLTCs) and capacitor banks (CBs) switching, are not flexible enough to mitigate the violations in the voltages. Since the voltage problem becomes increasingly critical, traditional voltage control methods are required to be improved or even fundamentally changed. Taking advantage of DGs that are close to the clients, more flexible and coordinated control methods are proposed to remove voltage violations.

The coordinated control of DGs can be realized using centralized and distributed approaches. However, the centralized approach relies on a central controller to contact all voltage-regulating devices inside. This approach requires a high investment of infrastructure, transparency of information, and reliability of communication [3]. While the distributed voltage control approach considers both local and global optimization based on local information and information shared by the neighbors. It uses limited information and communications to improve the overall performance [4]. Considering the significant number of DGs in an ADN, it is unreasonable to choose the centralized control approach. In addition, DGs may belong to different owners as microgrids [5] and are relatively concentrated. Therefore, it is reasonable to split the centralized control center into several distributed control centers. Some previous literature discussed the distributed control strategies for multi-microgrids. Reference [5] designed a hierarchical outage management scheme to enhance the resiliency of a distribution system containing multi-microgrids against extreme events. Reference [6] proposed a hierarchical and decentralized strategy to minimize the operational costs considering the microgrid controller's profit. In [7], a hierarchical interactive architecture was proposed for the multiple microgrids in a system while ensuring system stability and quality-of-service. Reference [8] defined a novel comprehensive index to resolve voltage/current control issues in multi-microgrid distribution systems. Reference [9] developed a distributed robust energy management scheme for multiple interconnected microgrids. Given these benefits, voltage control is also a main goal that is achievable through the distributed control of a multi-microgrid ADN.

The response speed of different voltage-regulating devices in an ADN are not the same. Some devices can respond to the instructions immediately, while others take longer to act. The Model Predictive Control (MPC) provides an effective solving method for multiple controller optimal coordination. It is suitable to solve the problem of coordinating diverse-speed controllers, as it considers the dynamic response process of the control variables using a multi-step optimization. The MPC has already been introduced into the control of power systems [10], [11]. Reference [12] applies the MPC to solve the voltage control problem of systems equipped with DGs and an LTC. The control scheme optimizes the operation of the controllers by considering the action delay. However, the strategy proposed in [12] does not ensure a voltage recovery speed that is as fast as the system can achieve. Thus, it is necessary to employ additional fast-speed capacity in extreme operation conditions. In addition, the cooperation of diverse-speed devices can be used to gain more fast-speed capacity in systems. Therefore, systems will rapidly handle the future voltage fluctuation.

This paper proposes a voltage control strategy for an ADN comprised of multi-microgrids based on a cooperative distributed MPC considering the economy and response speed. In this paper, the microgrid central controllers (MGCCs) identify the main characteristics after every specific interval and share these characteristics with the immediate neighbors. When a microgrid's voltage is out of bounds, it solves a voltage coordination problem instantly to coordinate the neighborhood resources in advance. Then, the preformed voltage changes of the immediate neighbors will be considered for microgrid scheduling optimization. In addition, a cooperative distributed MPC theory is implemented to schedule the microgrid local resources. By considering the future actions of slow-speed voltage regulating devices, the cooperation of diverse-speed devices maintains as much fast-speed regulating capacity reserve as possible. Compared with existing voltage control strategies, the key contributions of this paper are:

- The identified voltage regulation characteristics reflect the main characteristics of microgrids with various devices to limit the transmission of information among microgrids and reduce the dependency on transmission.
- The formulated voltage coordination problem can simultaneously coordinate the neighborhood resources according to their cost and speed of voltage control.
- The proposed microgrid scheduling strategy ensures a fast voltage control and maintains as much fast-speed regulating capacity reserve as possible.

The rest of this paper is organized as follows. The architecture of the proposed control scheme is shown in Section II. Section III identifies the voltage regulation characteristics of a microgrid. Subsequently, the voltage coordination model is formulated in Section IV. Section V presents the design of the microgrid scheduling optimization problem based on a cooperative distributed MPC. The proposed solution scheme is described in Section VI, numerical examples are discussed in Section VII, and Section VIII concludes the paper.

## II. GENERAL ARCHITECTURE OF THE PROPOSED VOLTAGE CONTROL SCHEME

In a multi-microgrid ADN, it is likely that microgrids are managed and operated under different ownership. Therefore, any voltage control scheme associated with such a system must consider the interests of every microgrid and should not restrict their autonomy. In addition, electrically close microgrids may have a greater effect on each other than distant microgrids. Therefore, this paper proposes a distributed voltage control framework where each microgrid communicates with its immediate neighbors. Considering the OLTC and CBs in an ADN are under the direct supervisory control of an automatic voltage control (AVC) system. The OLTC at the point of common coupling of the ADN may have significant impact on the voltage of all the microgrids in the feeder. Microgrids communicate with the AVC system when the neighbor resources are scarce. The AVC system transmits the voltage sensitivity matrix to the microgrids using offline power flow calculations at the interval of ultra-short term economic scheduling, which is typically 10 minutes [13]. The architecture of the multi-microgrid ADN contains information flow is depicted in Fig. 1.

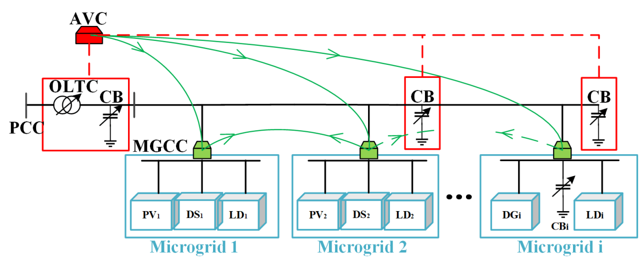


**FIGURE 1.** The architecture of the multi-microgrid ADN.

The voltage regulation characteristics transmitted between the microgrids includes an adjustable range, adjustment cost and regulating speed. The adjustable range defines the output power limits of the microgrid based on its current output. Since the R/X ratios of the cables at a medium-voltage ADN cannot be ignored, the change of the active power, which is supposed to be an expensive control variable, also plays an important role in voltage control in addition to the change of reactive power. Thus, the adjustment cost of the microgrid needs to be identified for coordination. Furthermore, the regulating speed of different voltage regulating devices are different, and the requirements regarding regulating the speed are different in different conditions. Microgrids identify the regulating speeds of the corresponding output power changes. The MGCCs then update and transmit information about the voltage regulation characteristics after each time interval of the ultra-short term economic scheduling. The specific formulas for the voltage regulation characteristics are discussed in detail in the following Section III. Fig. 2 demonstrates the information transmitted among the microgrids and the AVC system. The entire procedure of the proposed distributed voltage coordination strategy is presented in Table 1.

In this paper, the proposed voltage control strategy is triggered when the voltage of microgrids in ADN exceeds the limits. The distributed control framework is comprised of two stages. In the first stage, the microgrids in which a voltage violation occurs coordinate the neighborhood resources and calculate the initial values for distributed MPC according to the latest voltage regulation characteristics of their neighbors. If the voltage problem is serious, the MGCCs will require help from neighbors immediately and send the initial values to them. If the voltage problem does not imperil the safe operation, the MGCCs will concern whether the active power of neighbors is required. If the initial value of neighbors' active power is nonzero, it means that the reactive power capacity of neighbors is not enough to meet the voltage control demand. Then the MGCCs will ask the AVC system and neighbors for help. The AVC system participants in voltage control only when it is asked. And its action plan will be send to all microgrids in ADN.

Based on the initial values, the MGCCs compute values of their controllable variables and exchange information with their neighbors at the second stage. Each MGCC compares the results calculated by itself and the cooperation requests calculated by its neighbors at the first stage. The larger value will be selected as the initial values of distributed MPC to solve the microgrids scheduling problem. Then, the MGCCs will exchange their control sequence with their immediate neighbors. So that, each MGCC updates the control sequences computed in the previous iteration by its neighbors. The neighbors would apply the control sequences along the control horizon in case there were no further coordination updates. If convergence is reached or after the maximum number of iterations, the negotiation process is ending. Each MGCC applies the first entry of the control sequence to the microgrid. Fig. 3 shows the time progression of distributed MPC coordination procedure among three MGCCs.

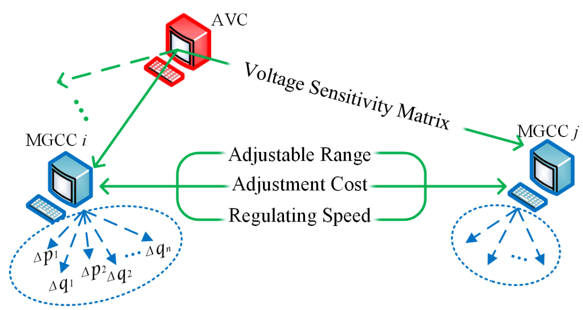


**FIGURE 2.** Information transmission architecture in the multi-microgrid ADN.

**TABLE 1.** Procedure of the proposed method.

| | |
|---|---|
| In normal conditions (Section III) | |
| *Step 1:* | The MGCCs calculate voltage regulation characteristics separately and exchange the information with immediate neighboring MGCCs at the interval of ultra-short term economic scheduling. |
| Once the voltage of microgrid $i$ is out of bounds Stage I: Voltage Coordination Problem (Section IV) | |
| *Step 2:* | The MGCC$_i$ instantly solves the voltage coordination problem considering the economy and response speed. |
| *Step 3:* | The MGCC$_i$ sends the coordination request to its immediate neighbors or asks the AVC system for help if necessary. |
| Stage II: Microgrid Scheduling Problem (Section V) | |
| *Step 4:* | The MGCCs select larger value of the results calculated by itself and its neighbors at the first stage as the initial values. |
| *Step 5:* | The MGCCs compute the control sequence by solving the microgrids scheduling problem. |
| *Step 6:* | The MGCCs exchange control sequence with their immediate neighbors. |
| *Step 7:* | If convergence is reached or if the maximum number of iterations is reached, proceed to Step 9. Otherwise, proceed to Step 5 |
| *Step 8:* | The MGCCs implement the first element of the control action sequences. |

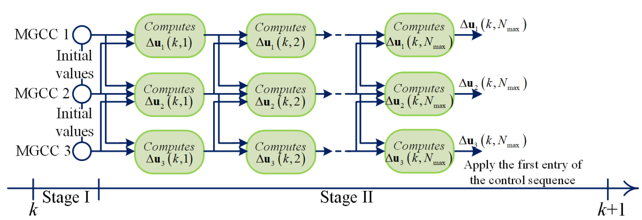


**FIGURE 3.** Schematic view of the time progression of distributed MPC coordination procedure after the maximum number of iterations $N_{\max}$.

## III. MICROGRID VOLTAGE REGULATION CHARACTERISTICS

### A. ADJUSTABLE RANGE

The adjustable range of a microgrid is related to the adjustable range of the controllable devices in that microgrid. Since the active power is only generated by DG units, the output limits of active power are as follows:

$$\Delta P^{\min} = \sum\nolimits_{n\in N} \left(p_n^{min} - p_n\right) \tag{1}$$

$$\Delta P^{\max} = \sum\nolimits_{n\in N} \left(p_n^{\max} - p_n\right) \tag{2}$$

where $p_n$ is the real-time output power of the DG unit $n$; $p_n^{min}$ and $p_n^{max}$ are the lower and upper limits of the DG unit $n$, respectively; and $\Delta P^{min}$ and $\Delta P^{max}$ are the lower and upper limits of the microgrid, respectively.

In addition, the DG units also provide reactive power like CBs. Distinct from the power electronics, the typical control of CBs is slow and discrete. According to the operational model of CBs [14], their adjustable range is formulated as follows:

$$\begin{cases} \Delta q = \Delta b_{n_b} q_{step,n_b} \\ \Delta b_{n_b} \in [-b_{n_b}, b_{n_b}^{\max} - b_{n_b}], \quad \Delta b_{n_b} \in ints \end{cases} \tag{3}$$

where $\Delta b_{nb}$ is the number of switching groups in $CB_{nb}$; $q_{step,nb}$ is the reactive power output of each group; $\Delta q$ is the change of the reactive power output provided by $CB_{nb}$; $b_{nb}$ is the switch status of $CB_{nb}$; and $b_{nb}^{max}$ is the maximum number of groups that $CB_{nb}$ can switch on.

Thus, the reactive power output limits of a microgrid are as follows:

$$\Delta Q^{\min} = \sum\nolimits_{n\in N} \left(q_n^{\min} - q_n\right) + \left(-b_{n_b}\right) q_{step,n_b} \tag{4}$$

$$\Delta Q^{\max} = \sum\nolimits_{n\in N} \left(q_n^{\max} - q_n\right) + \left(b_{n_b}^{\max} - b_{n_b}\right) q_{step,n_b} \tag{5}$$

where $q_n$ is the real-time output power of the DG unit $n$; $q_n^{min}$ and $q_n^{max}$ are the lower and upper limits of the DG unit $n$, respectively; and $\Delta Q^{min}$ and $\Delta Q^{max}$ are the lower and upper limits of the microgrid, respectively.

### B. ADJUSTMENT COST

The reactive power output of the DG units and the typical voltage regulating devices are considered cheap controls, while the active power output of the DG units is considered an expensive control. Therefore, the following discusses the microgrid adjustment cost of active power and reactive power separately.

During the coordination process, the microgrid may increase or decrease the active power output. The cost of active power output should be identified by the generation cost of the DG units in the microgrid. The cost of active power reduction $C^{com}$ is a fixed value. This value is equal to or slightly higher than the real-time grid electricity price to compensate the economic loss of the microgrid. The adjustment cost function $C(\Delta P)$ is formulated as:

$$C(\Delta P) = \begin{cases} C^P(\Delta P) \cdot \Delta P & \Delta P > 0 \\ C^{\text{com}} \left|\Delta P\right| & \Delta P < 0 \end{cases} \tag{6}$$

where $\Delta P$ is the active power change of the microgrid, $\Delta P < 0$ represents the power reduction, $\Delta P > 0$ represents the power generation, and $C^P(\Delta P)$ is the cost function of the power output increase.

In this context, the DG units are Photovoltaics (PVs) and Distributed Storage (DSs). Since PVs generally work in the MPPT mode, the real-time power output is the output limit under certain local weather conditions. Considering their output power cannot be increased, the cost function $C^P$ mainly relates to the DS. Their cost functions are assumed to be a quadratic function [15], [16]. The cost function of the DG unit $n$ is formulated as follows (see Fig. 4):

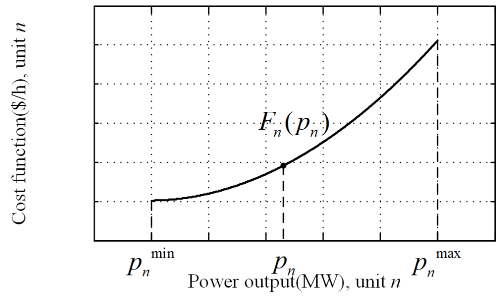


**FIGURE 4. Cost function of the DG unit n.**

$$F_n(p_n) = a_n p_n^2 + b_n p_n + c_n \tag{7}$$

where $p_n$ is the active power output of the DG unit $n$; $F_n(p_n)$ is the cost of the DG unit $n$; and $p_n$, $b_n$, $c_n$ are cost coefficients of the DG unit $n$.

The first derivative of the cost function is the incremental cost $C_{n,t}^P$ of the $DG_n$ at instant $t$:

$$C_{n,t}^P = \left.\frac{dF_n(p_n)}{dp_n}\right|_{p_n=p_{n,t}} = 2a_n p_{n,t} + b_n \tag{8}$$

where $p_{n,t}$ represents the active power output $DG_n$ at instant $t$.

It is assumed that the active power output of the $DG_n$ increases from $P_{n,t'}$ at instant $t$ to $p_{n,t'}$ at instant $t$'. Then, the incremental cost is calculated as Equation (9).

$$C_{n,t'}^P = 2a_n p_{n,t'} + b_n \tag{9}$$

The change in the output power is expressed in Equation (10). Substituting Equation (10) into Equation (9), the incremental cost at instant $t'$ is formulated as Equation (11).

$$\Delta p_n = p_{n,t'} - p_{n,t} \tag{10}$$

$$C_{n,t'}^P = 2a_n\left(p_{n,t} + \Delta p\right) + b_n = 2a_n \Delta p_n + C_{n,t}^P \tag{11}$$

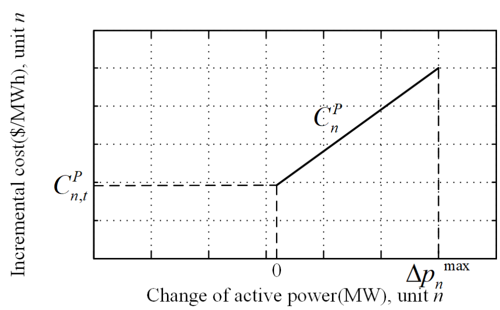


**FIGURE 5. Incremental cost curve of the DG unit n.**

The incremental cost of $\Delta p_n$ is related to the incremental cost of the $DG_n$ at instant $t$, as shown in Fig. 5. Performing the sum at equal ordinates to the incremental cost of all DG units [17], we obtain the microgrid incremental cost of the $\Delta P$ (see Fig. 6).

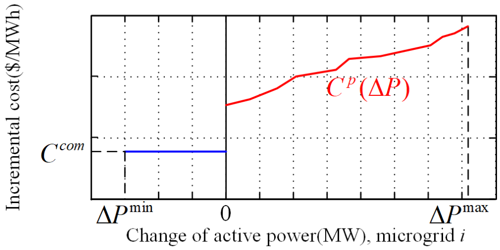


**FIGURE 6. Microgrid incremental cost curve of the active power.**

Distinct from active power, the cost of reactive power is usually ignored in current studies. In this context, to obtain more active coordination in reactive power, the microgrid that needs voltage support must compensate the neighboring microgrids providing the reactive power during coordination [18]. The cost of reactive power $C^Q$ is set as a fixed value that is far less than the unit cost of active power. The adjustment cost function $C(\Delta Q)$ is formulated as:

$$C\left(\Delta Q\right) = C^{Q}\left|\Delta Q\right| \tag{12}$$

where $\Delta Q$ is the reactive power change in the microgrid.

### C. REGULATING SPEED

Since the active power of the DG changes within milliseconds, the regulating time is negligible relative to the control interval. Therefore, it is feasible to regard the active power regulating as instantaneous regulating. In contrast, the reactive power is regulated using different voltage regulating devices with different regulating speeds. When the voltage problem is serious, the fast-speed regulating devices should be invoked first. The slower-speed regulating devices are called only when there is no faster regulating capacity. Therefore, this paper sums the available faster-speed capacity first and then adds the slower-speed capacity to obtain the microgrid response delay of $\Delta Q$ (see Fig. 7).

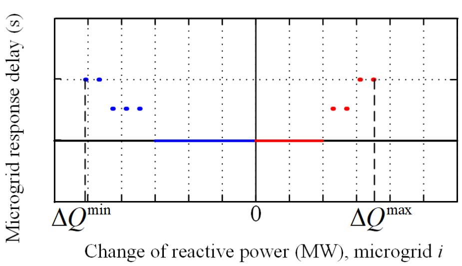


**FIGURE 7. Microgrid response delay curve for the reactive power.**

When the value of $\Delta Q$ is small, the change in the reactive power is continuous and rapid. With the increasing requirements of $\Delta Q$, the fast speed reactive power reserve in the microgrid is exhausted. Under this circumstance, the change in the reactive power is discrete and slow. Therefore, the requirements of $\Delta Q$ are smaller, the regulating speed is faster, and the regulating performance is better. If there are multiple immediate neighboring microgrids that participate in the regulation, it is feasible to reduce the reactive power requirement of a single microgrid and allocate the reactive power requirement among each of them to speed up the voltage regulation process.

## IV. VOLTAGE COORDINATION PROBLEM

In this paper, the voltage coordination is triggered only when the voltage violates the predefined limits. The microgrid in which the voltage violation occurs takes the role of the coordinator. Considering the neighboring voltage regulation characteristics, it calculates the voltage change target of its neighbors immediately and balances the adjustment cost and regulating speed based on the severity of the voltage violation.

This problem is a voltage coordination problem. Its objectives are to minimize the adjustment cost and accelerate the regulating speed while satisfying the voltage limits. It leads to the following standard quadratic programming problem:

$$\min(\left\|\boldsymbol{C}^{P}\Delta\boldsymbol{P}^{T}\right\|_{WP}^{2} + \left\|C^{Q}\Delta\boldsymbol{Q}^{T}\right\|_{WQ}^{2}) \tag{13}$$

subject to:

$$\Delta\boldsymbol{P}^{\min} \leq \Delta\boldsymbol{P} \leq \Delta\boldsymbol{P}^{\max} \tag{14}$$

$$\Delta\boldsymbol{Q}^{\min} \leq \Delta\boldsymbol{Q} \leq \Delta\boldsymbol{Q}^{\max} \tag{15}$$

$$V_{i}^{\min} \leq V_{i} + \Delta V_{i} \leq V_{i}^{\max} \tag{16}$$

$$\Delta V_{i} = \frac{\partial V_{i}}{\partial \boldsymbol{P}}\Delta\boldsymbol{P} + \frac{\partial V_{i}}{\partial \boldsymbol{Q}}\Delta\boldsymbol{Q} \tag{17}$$

where $\Delta\boldsymbol{P}$ and $\Delta\boldsymbol{Q}$ are the vectors that represent the changes of output power of itself and its neighbors and are defined as $\Delta\boldsymbol{P} = [\Delta P_i, \Delta P_{j1}, \Delta P_{j2}, \ldots, \Delta P_j]^{\mathrm{T}}$ and $\Delta\boldsymbol{Q} = [\Delta Q_i, \Delta Q_{j1}, \Delta Q_{j2}, \ldots, \Delta Q_j]^{\mathrm{T}}$. The $\boldsymbol{C}^P$ is a vector and $C^Q$ is a constant, which represent the cost of the active and reactive power, respectively. The weighting matrices $\boldsymbol{WP}$ and $\boldsymbol{WQ}$ have different values according to different urgency levels of the voltage problem.

### A. WEIGHTING CALCULATION

The weight assigned to each control variable directly influences the cost and speed of the coordination performance. According to the predefined limits, the voltages can be divided into the dead zone, uneconomic zone and emergency zone, as shown in Fig. 8. The upper and lower normal operating limits are $V_{ec}^{max}$ and $V_{ec}^{min}$, respectively, and the upper and lower emergency limits are $V_{em}^{max}$ and $V_{em}^{min}$, respectively.

The values between $V_{ec}^{min}$ and $V_{ec}^{max}$ are in the dead zone. This zone means that the system is under the optimum operation. The values in $[V_{ec}^{max}, V_{em}^{max}]$ and $[V_{em}^{min}, V_{ec}^{min}]$ are in the uneconomic zone. When voltages fall in this zone, the operating cost of the system and microgrids increases, but will not affect the security of the system. In this condition,

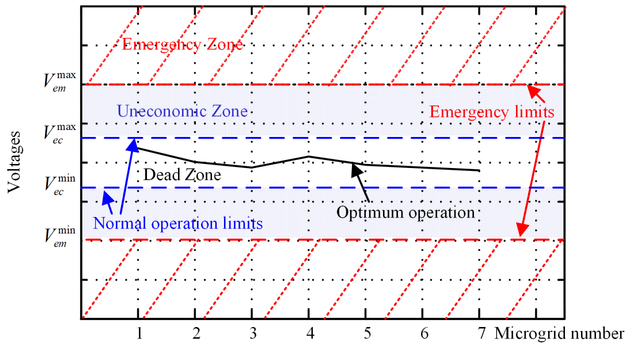


**FIGURE 8.** Schematic diagram of the operation zones.

microgrids should adjust voltages to reduce deviation from the optimal operation conditions. The main consideration of microgrids is the adjustment cost. If values are outside the emergency limits, they are in the emergency zone, and the system reliability and security cannot be guaranteed. Therefore, voltage coordination scheduling will correct the voltages back to dead zone or uneconomic zone as fast as possible. In this condition, the neighbor that has more fast-speed power capacity should be given more priority in the coordination process. This process pays more attention to regulating speed than adjustment cost.

Therefore, the value of weighting matrices ***WP*** and ***WQ*** are determined as follows:

1) If the voltages are in the uneconomic zone, the associated microgrids will coordinate recourse of neighborhood to regulate voltages with minimum cost. Thus, the value of the matrix ***WP*** elements should be larger than that of the matrix ***WQ*** elements to minimize the use of expensive active power.
2) Once the voltages are outside the emergency limits, the associated microgrids will be more inclined to use the fast response capacity. The elements in the matrix ***WQ*** associated with the microgrids that have more fast-speed capacity should be smaller than the other elements. In addition, the values of the matrix ***WP*** should be reduced for more available fast-speed resources.

## B. SENSITIVITY MATRIX CALCULATION

After solving the voltage coordination problem, the microgrid determines whether it needs help from neighboring microgrids and the voltage change target of each neighbor. The voltage change target of microgrid j can be calculated as follows:

$$\Delta V_{ij}^{ref} = \frac{\partial V_j}{\partial P_j}\Delta P_j + \frac{\partial V_j}{\partial Q_j}\Delta Q_j \tag{18}$$

The accurate sensitivity matrix should incorporate the network impedances in the microgrids and the specific output of each DG. However, it is not feasible to obtain this information in application, considering that the DGs in a microgrid are relatively concentrated. This paper chooses a typical node in a microgrid that can represent the internal voltage level of the microgrid. The microgrid internal voltage operating status can be reflected by monitoring this node, and the accurate sensitivity matrix can be approximated by the sensitivity of the typical node. The voltage sensitivity of the typical node can be calculated from the inverse of the Jacobian matrix, which is defined from the offline power flow calculation [19].

## V. MICROGRIDS SCHEDULING PROBLEM

The word "data" is plural, not singular.

The microgrid strategic scheduling lies in optimally scheduling the internal devices, such as the PV, DS, and equipped CBs, to meet the voltage deviation demanded of itself and its neighbors. Meanwhile, the microgrid scheduling minimizes the adjustment cost, accelerates the regulating speed and maximizes the fast-speed power reserve.

The difficulty of the microgrid scheduling is rooted in the cooperation of the diverse-speed regulating devices. In this paper, it is assumed that the slow-speed regulating devices receive instructions at one moment and execute instructions at another. In contrast, the fast-speed regulating devices take action instantly the moment they receive instructions. A multi-step optimization based on the distributed MPC theory is optimal to handle the microgrid scheduling problem. Utilizing distributed MPCs allows consideration of the actions of slow-speed regulating devices in a future period and leads the MGCC to give out instructions in advance. At the same time, the available fast-speed power reserve capacity can be increased at the end of the predictive horizon.

After receiving the voltage coordination request from the neighboring microgrids, the MGCC needs to dispatch the controllable devices according to the requested voltage reference to realize economical and rapid voltage control. In addition to assisting its neighbors, a microgrid may also encounter voltage problem of its own. That is, its optimization objective will take into account the regulating target of itself and its neighbors. Therefore, the optimization problem of microgrid scheduling over the control horizon can be formulated as below:

$$\begin{aligned}\min \sum_{t=k+1}^{k+N_C} \sum_{j\in Z^i} \alpha_j \left\| V_{j,t} - V_{j,t}^{ref} \right\|_{Q_{ij}}^2 + \sum_{t=k+1}^{k+N_C} \left\| \tan\theta_{PV,t} - 1 \right\|_{Q_\theta}^2 \\ + \sum_{t=k+1}^{k+N_C} \left( \left\| \sum_{n_b=1}^{N_{CB}} C^Q \left| q_{n_b,t} \right| \right\|_{R_s}^2 \right. \\ \left. + \left\| \sum_{n=1}^{N} \left( F_n\left(p_{n,t}\right) + C^Q \left| q_{n,t} \right| \right) \right\|_{R_c}^2 \right)\end{aligned} \tag{19}$$

subject to:

$$p_{n,t}^{\min} \le p_{n,t} \le p_{n,t}^{\max} \tag{20}$$

$$q_{n,t}^{\min} \le q_{n,t} \le q_{n,t}^{\max} \tag{21}$$

$$q_{n,t}^{\max} = -q_{n,t}^{\max} = p_{n,t} \tan\theta_n \tag{22}$$

$$soc_n^{\min} \le soc_n \le soc_n^{\max} \tag{23}$$

$$q_{n_b,t} = b_{n_b,t} q_{n_b,step}, \quad b_{n_b,t} \leq b_{n_b,t}^{\max} \tag{24}$$

$$V_{i,t}^{\min} \leq V_{i,t} \leq V_{i,t}^{\max} \tag{25}$$

$$V_{i,k+1} = V_{i,k} + \mathbf{S}_1 \Delta \mathbf{u}_{1,k} + \mathbf{S}_2 \Delta \mathbf{u}_{2,k-\tau} + \sum_{j \in Z^i} \Delta V_{ij} \tag{26}$$

where $N_C$ is the length of the control horizon; $Z^i$ is the set of microgrid $i$ and its neighbors. $V_{j,t}$ is the predicted voltage of the microgrid $j$ at the time instant $t$; $V^{ref}$ is the reference value of voltage; $k$ is the discrete time instant; $N_{CB}$ is the number of CBs in a microgrid; and $N$ is the number of DGs in a microgrid.

The first term in Equation (19) represents the voltage deviation from the voltage target. If the voltage of microgrid $j$ is out of the limits, $\alpha_j = 1$; otherwise, $\alpha = 0$. The second term represents PV power factor deviation from the MPPT mode. The third terms account for the operational cost of controllable units in the microgrid.

The variable $V_{i,t}$ in constraint Equation (25) is calculated using Equation (26) so that the actions of diverse-speed regulating devices can be considered in the optimization problem. Then, Equation (26) formulates the voltage prediction model considering diverse-speed regulating devices. The matrix $\boldsymbol{S}$ is the voltage sensitivity of the internal controllable nodes. The $\boldsymbol{u}_1$ and $\boldsymbol{u}_2$ are the fast and slow control variables, respectively, and $\tau$ is the execution delay time. The $\Delta V_{ij}$ should be updated by communicating the variable changes with its neighbors at every control interval.

## VI. SIMULATION RESULTS

### A. DESCRIPTION OF THE TEST SYSTEM

Simulation studies are carried out on a multi-microgrid active distribution network comprised of three microgrids, as shown in Fig. 9. The multi-microgrid ADN system is connected to the external grid through a 110/10 kV transformer OLTC. Microgrid 1 is a factory equipped with fast-speed regulating devices, PV and two different DSs and slow-speed regulating devices, CBs. Microgrid 2 is a shopping mall possessing PV and DS. Microgrid 3 is a residential community containing PV and DS. The AVC system contains the OLTC and CBs. The load profiles of the three microgrids are of the industrial, commercial, and residential types, respectively.

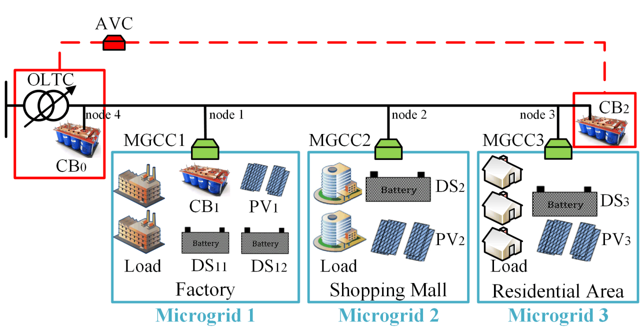


**FIGURE 9.** The structure of the simulation system.

The maximum annual output powers of the PV are 2 MWp, 1 MWp, and 1 MWp, respectively.

**TABLE 2.** Line parameter values.

| Node $i$ | Node $j$ | r/Ω | x/Ω | b/S | Ratio |
|---|---|---|---|---|---|
| 1 | 4 | 2.47 | 1.96 | 0 | 1 |
| 1 | 2 | 3.01 | 2.26 | 0 | 0 |
| 2 | 3 | 2.58 | 2.87 | 0 | 0 |

The transmission line parameters are summarized in Table 2. The parameters associated with DSs are specified in Table 3. The parameters associated with OLTC and CBs are specified in Table 4. Various case studies are presented to examine the features of the proposed strategy.

**TABLE 3.** Energy storage unit characteristics.

| *unit* | *a* | *b* | *c* | $p^{max}$ (kW) | $p^{min}$ (kW) |
|---|---|---|---|---|---|
| $DS_{11}$ | 0. 040 | 27 | 0 | 400 | -200 |
| $DS_{12}$ | 0. 035 | 22 | 2 | 600 | -300 |
| $DS_2$ | 0. 037 | 23 | 8 | 800 | -400 |
| $DS_3$ | 0. 032 | 19 | 0 | 1000 | -500 |

**TABLE 4.** Conventional voltage regulating unit characteristics.

| *unit* | $\tau$ | $l^{min}$, $l^{max}$ | $b^{max}$ | $\Delta V_{tap}$ | $q_{step}$ |
|---|---|---|---|---|---|
| *OLTC* | 10 s | -8, +8 | / | 1.875% | / |
| $CB_{0,1,2}$ | 5 s | / | 3 | / | 334kvar |

The values of upper and lower normal operating limits are 1.03 p.u. and 0.97 p.u., respectively. The values of upper and lower emergency limits are 1.05 p.u. and 0.95 p.u., respectively. The cost of active power reduction is 0.03 \$/kW. The cost of reactive power $C^Q$ is set as 0.002 \$/kvarh. Minimum power factor of inverter during voltage control is 0.99. Predictive horizon is 30s and control horizon is 15s, the control interval is 5s. Iteration precision of distributed MPC is 0.005 and the maximum number of iteration times is 10. The MGCCs use the commercial solver Gurobi of YALMIP toolbox to solve the optimization problems.

### B. RESULTS AND ANALYSIS

*Case 1:* Coordination of microgrids and AVC system.

This case usually occurs in the midafternoon, where the industrial load in microgrid 1 and the commercial load in microgrid 2 are at the peak while residential load of microgrid 3 is at a low level. At the initial time, the active power output of PV is approximately 0.6 p.u. and two groups of the $CB_1$ and one group of $CB_2$ have been connected to the system to maintain the normal operation of the ADN. At time 2s, due to the weather, the PVs power output of are suddenly decreased to 0.5 p.u. which undoubtedly leads to a sudden voltage dip of each microgrid (see Fig. 10). The voltage of microgrid 1 and microgrid 3 remains within the bounds of normal operation, while the voltage of microgrid 2 exceeds

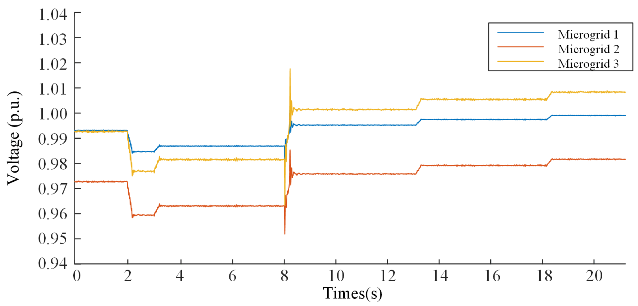


**FIGURE 10.** Voltage correction for case 1.

the lower limit of normal operating range which requires voltage control. Therefore, only the MGCC2 needs to solve voltage coordination problem in stage I. The results of stage I are listed in Table 5. The change of reactive power in microgrid 1 contains the reactive capacity of the slow-speed regulating devices CBs.

**TABLE 5.** Results of stage I calculated by microgrid 2.

| | $\Delta P$(kW) | $\Delta Q$ (kvar) |
|---|---|---|
| Microgrid 1 | 0 | 172.6 |
| Microgrid 2 | 9.6 | 69.6 |
| Microgrid 3 | 13.7 | 69.6 |

The results indicate that the more expensive active capacity is used which means reactive capacity of microgrid 2 and its neighbors cannot meet the voltage regulation requirements. Considering the voltage of microgrid 2 is not in the emergency zone, changing active power of neighbors is not the economic decision. Therefore, microgrid 2 sends out voltage requests to its neighbors and as well the AVC system.

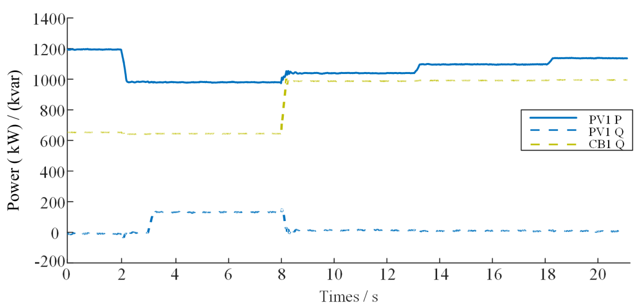


**FIGURE 11.** Power output of the devices in microgrid 1 for case 1.

Fig. 11 and Fig. 12 shows the cooperation process of the slow-speed regulating device, CBs, and the fast-speed regulating devices, PVs. At time 3s, the PVs immediately injected reactive power to the bus to raise the voltage. At the same time, the CBs received instructions from the MGCC3. However, the CBs did not act until 5s later because of its execution delay. The reactive power of the PV drops down as soon as the CBs acted. Due to the action of the CBs, there are

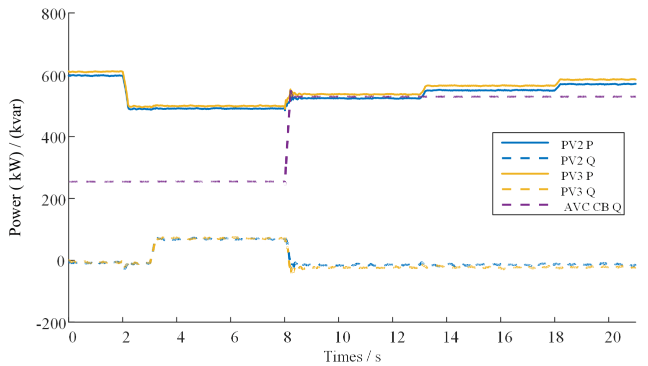


**FIGURE 12.** Power output of the devices in microgrid 2 and 3 for case 1.

twice transient oscillations fluctuations that occurred at 8 s. Their amplitudes are in the acceptable range. In this case, the DS in microgrid 1 did not generate power to support the voltage because the DS reactive power output is limited by the power factor, and its initial active power output is zero.

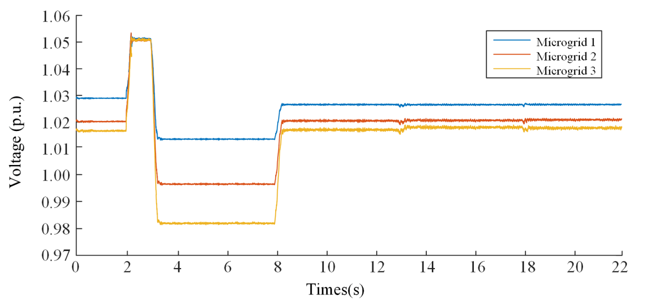


**FIGURE 13.** Voltage correction for case 2.

*Case 2:* Coordination of multi-microgrids.

The case usually happens in the morning, where the industrial load in microgrid 1 and the commercial load in microgrid 2 are at a low level while residential load of microgrid 3 is ascending to a small peak. At time 2s, the voltages of microgrids face over voltage condition because of the PV active power increment, which arose from weather changes. Due to the general low load level of the ADN at this time, the sudden increase of PV output has led to an abrupt rise in voltages (see Fig. 13). The voltage of microgrid 3 exceeds the upper emergency limit which requires emergency control. Meanwhile, the voltages of microgrid 1 and microgrid 2 are outside of the uneconomic zone which also need to carry out voltage control. Therefore, the three MGCCs start to solve voltage coordination problem immediately. Although microgrid 1 and microgrid 2 are in the similar voltage situation, the results of them are very different. The results calculated by microgrid 1 indicate that the reactive capacity of itself and its neighbors are still not enough to meet the voltage constraints. Thus, microgrid 1 will also change the active power of itself. Since the voltages of microgrid 3 are outside the emergency limit, it must regulate their voltages as fast as possible by changing active power. The results of stage I are listed in Table 6. The change of reactive power in microgrid 1 contains the reactive capacity of the slow-speed regulating devices CBs. Each MGCC transmits its voltage requests to its neighbors and enters stage II.

**TABLE 6.** Results of stage I.

| | $\Delta P$(kW) | $\Delta Q$ (kvar) |
|---|---|---|
| CALCULATED BY MICROGRID 1 | | |
| Microgrid 1 | -0.1316 | -0.5243 |
| Microgrid 2 | 0 | -0.0951 |
| CALCULATED BY MICROGRID 2 | | |
| Microgrid 1 | 0 | -0.4882 |
| Microgrid 2 | 0 | -0.0951 |
| Microgrid 3 | 0 | -0.1021 |
| CALCULATED BY MICROGRID 3 | | |
| Microgrid 2 | -0.0000 | -0.0951 |
| Microgrid 3 | -0.1055 | -0.1021 |

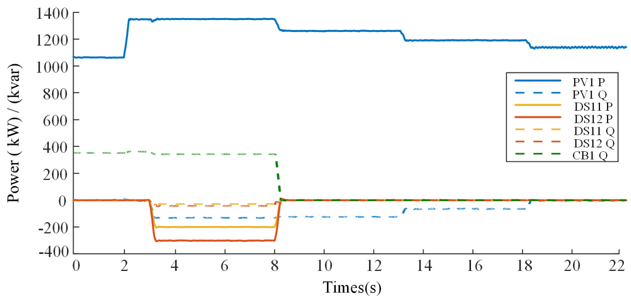


**FIGURE 14.** Power output of the devices in microgrid 1 for case 2.

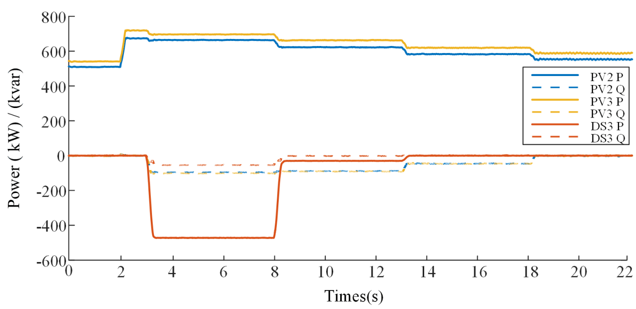


**FIGURE 15.** Power output of the devices in microgrid 2 and 3 for case 2.

After the distributed solution of stage II, the control results of variables in three microgrids are shown in Fig. 14 and Fig. 15. According to the control instructions, at time 3s, the PVs reactive power are reduced to the minimum value limited by the power factor. Meanwhile, the DSs change into the charging state, at time 8s, with the action of $CB_1$, the DSs charging power are gradually return to zero and the PVs reactive power are gradually reducing and going back to zero when voltages are stable within normal operating range. The action of $CB_1$ reduces the system operation cost and retains more capacity of fast-speed regulating devices in the system.

In this case, fast-speed devices take actions immediately to solve the urgent voltage problem immediately and meanwhile the MGCC sends instructions to the slow-speed devices at the same time. After the action of slow-speed devices, a part of the rapid response capacity is released. Based on the distributed MPC, the fast-speed and relatively expensive variables can be reduced gradually with the input of cheap slow-speed variables, which not only reduces the control cost but also increases the fast-speed power reserve to face potential voltage problems in the future.

## VII. CONCLUSION

This paper has presented a novel distributed control of multi-microgrid ADNs for rapidly regulating of voltages with a minimum operating cost. The microgrid voltage regulation characteristics were established to limit the amount of information transmitted. According to these characteristics, MGCCs coordinate neighbors' resources appropriately for voltage regulation. Then a cooperative distributed MPC theory is implemented to schedule the microgrid local resources considering the future actions of slow-speed voltage regulating devices. This ensures fast voltage regulating performance and maintains as much fast-speed regulating capacity reserve as possible.

Simulations regarding the ADN comprised of three microgrids demonstrates that the proposed strategy can eliminate voltage violations economically and rapidly with an effective coordination of the diverse-speed regulating devices.

## REFERENCES

[1] J. Tengku, A. Mohamed, H. Shareef, "A review on voltage control methods for active distribution networks," *Przeglad Elektrotechniczny*, vol. 88, pp. 304–312, Jun. 2012.

[2] R. Tonkoski and L. A. C. Lopes, "Impact of active power curtailment on overvoltage prevention and energy production of PV inverters connected to low voltage residential feeders," *Renew. Energy*, vol. 36, pp. 3566–3574, Dec. 2011.

[3] Y. Liu, H. Gao, J. Liu, Z. Ma, J. Chen, and Y. Yang, "Multi-agent based hierarchical power scheduling strategy for active distribution network," in *Proc. Int. Symp. Smart Elect. Distribution Syst. Technol. (EDST)*, 2015, pp. 151–158.

[4] R. R. Negenborn and J. M. Maestre, "Distributed model predictive control: An overview and roadmap of future research opportunities," *IEEE Control Syst.*, vol. 34, no. 4, pp. 87–97, Aug. 2014.

[5] H. Farzin, M. Fotuhi-Firuzabad, and M. Moeini-Aghtaie, "Enhancing power system resilience through hierarchical outage management in multi-microgrids," *IEEE Trans. Smart Grid*, vol. 7, no. 6, pp. 2869–2879, Nov. 2016.

[6] V. Bui, A. Hussain, and H.-M. Kim, "A multiagent-based hierarchical energy management strategy for multi-microgrids considering adjustable power and demand response," *IEEE Trans. Smart Grid*, vol. 9, no. 2, pp. 1323–1333, Mar. 2018.

[7] D. Li and S. K. Jayaweera, "Distributed smart-home decision-making in a hierarchical interactive smart grid architecture," *IEEE Trans. Parallel Distrib. Syst.*, vol. 26, no. 1, pp. 75–84, Jan. 2015.

[8] S. A. Arefifar, M. Ordonez, and Y. A. R. I. Mohamed, "Current controllability in multi-microgrid smart distribution systems," *IEEE Trans. Smart Grid*, vol. 9, no. 2, pp. 817–826, Mar. 2018. doi: 10.1109/TSG.2016.2568999.

[9] Y. Liu *et al.*, "Distributed robust energy management of a multi-microgrid system in the real-time energy market," *IEEE Trans. Sustain. Energy*, to be published. [Online]. Available: https://ieeexplore.ieee.org/document/8141420/, doi: 10.1109/TSTE.2017.2779827.
[10] B. Otomega, M. Glavic, and T. Van Cutsem, "A two-level emergency control scheme against power system voltage instability," *Control Eng. Pract.*, vol. 30, pp. 93–104, Sep. 2014.
[11] M. Moradzadeh, R. Boel, and L. Vandevelde, "Voltage coordination in multi-area power systems via distributed model predictive control," *IEEE Trans. Power Syst.*, vol. 28, no. 1, pp. 513–521, Feb. 2013.
[12] G. Valverde and T. Van Cutsem, "Model predictive control of voltages in active distribution networks," *IEEE Trans. Smart Grid*, vol. 4, no. 4, pp. 2152–2161, Dec. 2013.
[13] L. A. Tuan and K. Bhattacharya, "Competitive framework for procurement of interruptible load services," *IEEE Trans. Power Syst.*, vol. 18, no. 2, pp. 889–897, May 2003.
[14] Z. Li, W. Wu, B. Zhang, H. Sun, and Q. Guo, "Dynamic economic dispatch using Lagrangian relaxation with multiplier updates based on a quasi-Newton method," *IEEE Trans. Power Syst.*, vol. 28, no. 4, pp. 4516–4527, Nov. 2013.
[15] T. A. Nguyen and M. L. Crow, "Stochastic optimization of renewable-based microgrid operation incorporating battery operating cost," *IEEE Trans. Power Syst.*, vol. 31, no. 3, pp. 2289–2296, May 2016.
[16] C. Long and L. F. Ochoa, "Voltage control of PV-rich LV networks: OLTC-fitted transformer and capacitor banks," *IEEE Trans. Power Syst.*, vol. 31, no. 5, pp. 4016–4025, Sep. 2016.
[17] U. Fragomeni, "Direct method to multi-area economic dispatch," in *Proc. Int. Conf. Adv. Power Convers. Energy Technol. (APCET)*, Mylavaram, India, 2012, pp. 1–5.
[18] A. D. Papalexopoulos and G. A. Angelidis, "Reactive power management and pricing in the California market," in *Proc. IEEE Medit. Electrotech. Conf. (MELECON)*, May 2006, pp. 902–905.
[19] A. Borghetti *et al.*, "Short-term scheduling and control of active distribution systems with high penetration of renewable resources," *IEEE Syst. J.*, vol. 4, no. 3, pp. 313–322, Sep. 2010.

**XIAOBO DOU** (M'11) received the B.S.E.E. degree from Hohai University, Nanjing, China, in 2001, and the Ph.D. degree from Southeast University, Nanjing, China, in 2006.

He is currently a Professor with the School of Electrical Engineering, Southeast University. His current interests include smart grid, microgrid, and renewable energy resources.

**PEI XU** received the B.Sc. degree in electrical engineering from Southeast University, Nanjing, China, in 2015, where she is currently pursuing the M.Sc. degree in electrical engineering.

Her current research interests mainly include active distribution network control.

**QINRAN HU** (S'11–M'15) received the B.S. degree from Chien-Shiung Wu Honors College, Southeast University, China, in 2010, and the M.S. and Ph.D. degrees from the University of Tennessee, Knoxville, TN, USA, in 2013 and 2015, respectively.

He is currently a Post-Doctoral Fellow with Harvard University, Cambridge, MA, USA. His current research interests include power system optimization, behavioral demand response, and electricity market design.

**WANXING SHENG** (M'11–SM'14) received the B.Sc., M.Sc., and Ph.D. degrees from Xi'an Jiaotong University, Xi'an, China, in mechanical engineering. Since 1997, he has been a Full Professor with the China Electric Power Research Institute, Beijing, China, where he is currently the Head of the Department of Power Distribution. He is also a Leader of intelligent distribution system and an Excellent Expert with the State Grid Corporation of China.

He has authored over 150 refereed journal and conference papers and 15 books. He has also completed numerous state-funded research and development projects as a Principal Investigator. His research interests include power system analysis and automation, renewable energy, and smart grid integration.

**XIANGJUN QUAN** (S'16) received the B.S.E.E. degree in power systems and its automation from Chongqing University, Chongqing, China, in 2007, and the M.S. degree in power systems and its automation from Southeast University, Nanjing, China, in 2014, where he is currently pursuing the Ph.D. degree in advanced control of the interface inverter for the distributed generation.

In 2017, he was with the FREEDM Systems Center, North Carolina State University, Raleigh, NC, as an Exchanging Student. Since 2017, he has been with The University of Texas at Austin, Austin, TX, USA, as an Exchange Student. His current research interests include digital control technique for converters, renewable energy generation systems, and microgrid.

**ZAIJUN WU** (M'18) received the B.Eng. degree in power system and its automation from the Hefei University of Technology, Hefei, China, in 1996, and the Ph.D. degree in electrical engineering from Southeast University, Nanjing, China, in 2004.

He was a Visiting Scholar with The Ohio State University, USA, from 2012 to 2013. He is currently a Professor with the School of Electrical Engineering, Southeast University. His research interests include substation automation, microgrid, and power quality. He has authored or co-authored about 60 referred journal papers. He is a reviewer of several journals.

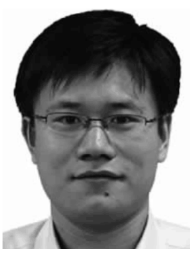

**BIN XU** is currently with the State Grid Anhui Electric Power Corporation Research Institute, Hefei, China. His research interests include active distribution network and power system operation.